A Preliminary Review of Global CO$_2$ Exchange Between Ocean and Atmosphere

R. Davis
M. Gregg

March 8, 1993

JSR-90-302

REPORT DOCUMENTATION PAGE

1. AGENCY USE ONLY (Leave blank)	2. REPORT DATE March 16, 1993	3. REPORT TYPE AND DATES COVERED

4. TITLE AND SUBTITLE	5. FUNDING NUMBERS
A Preliminary Review of Global CO_2 Exchange Between Ocean and Atmosphere	PR - 8503A
6. AUTHOR(S) R. David, M. Gregg	

7. PERFORMING ORGANIZATION NAME(S) AND ADDRESS(ES) The MITRE Corporation JASON Program Office A10 7525 Colshire Drive McLean, VA 22102	8. PERFORMING ORGANIZATION REPORT NUMBER JSR-90-302

9. SPONSORING/MONITORING AGENCY NAME(S) AND ADDRESS(ES) Department of Defense Washington, DC 20301-7100	10. SPONSORING/MONITORING AGENCY REPORT NUMBER JSR-90-302

11. SUPPLEMENTARY NOTES

12a. DISTRIBUTION/AVAILABILITY STATEMENT Approved for public release; distribution unlimited	12b. DISTRIBUTION CODE

13. ABSTRACT (Maximum 200 words)

This report examines issues concerning the determination of the exchange of CO_2 between the ocean and the atmosphere.

14. SUBJECT TERMS		15. NUMBER OF PAGES
carbon chemistry, turbulent fluxes, bulk fluxes		16. PRICE CODE

17. SECURITY CLASSIFICATION OF REPORT	18. SECURITY CLASSIFICATION OF THIS PAGE	19. SECURITY CLASSIFICATION OF ABSTRACT	20. LIMITATION OF ABSTRACT
UNCLASSIFIED	UNCLASSIFIED	UNCLASSIFIED	SAR

Contents

1 INTRODUCTION

Although the present rate of increase of CO_2 in the atmosphere is well documented, changes in the next century cannot be accurately predicted because the CO_2 budget is so poorly understood. The atmospheric concentration is increasing 1.4 ppm/year, corresponding to an increase in the atmospheric inventory of 3 Gt/year (1 Gt is 10^9 metric tons or 10^{12} kg). This observed increase is less than half of the estimated 8.7 Gt/year released by all sources to the atmosphere [10]. Most of the residual has been assumed to enter the ocean [15]. This cannot be verified directly, however, since the total dissolved inorganic CO_2 in the ocean is so much larger than the cumulative release of fossil fuel since 1850 that the change due to fossil fuel is small compared to natural variability. As a result, global CO_2 budgets are attempted by calculating the fluxes between ocean and atmosphere and between land and atmosphere.

There are two approaches to CO_2 fluxes between ocean and atmosphere. The first, widely used in geochemical studies, uses bulk formulas based on the difference of the partial pressure of CO_2 denoted pCO_2, between air and water, and on U_{10}, the wind speed 10 m above the sea surface. The bulk approach is not well established, however, and differences exist in the formulas, in methods of measuring partial pressures, and in the spatial and temporal coverage of the data used to evaluate the formulas. Consequently, global calculations of net CO_2 fluxes also vary widely. The second approach to CO_2 fluxes, developed by boundary layer turbulence investigators, is more recent

and utilizes new fast-responding detectors for CO_2 concentration. These are necessarily point measurements, but similar direct measurements of heat and water vapor fluxes have been used to develop and validate bulk formulas for those variables. Although the instrumentation is still being developed, the results seem consistent with the more traditional measurements of water vapor and heat fluxes. The direct CO_2 measurements, however, give fluxes much larger than bulk formulas used by the geochemists, producing vigorous controversy.

Before considering how the fluxes are estimated, the treatment by Broecker and Peng [14] is summarized to provide some background about the chemistry of carbon dissolved in the sea.

2   CARBON CHEMISTRY

Carbon dioxide gas crosses the sea surface primarily because of the reaction

$$H_2O + CO_2 + CO_3^= \rightleftharpoons 2HCO_3^- , \qquad (2-1)$$

where $CO_3^=$ is the carbonate ion and HCO_3^- is the bicarbonate ion. Without this reaction, CO_2 would exist in the upper ocean only as dissolved gas, and the ocean would take up only 3% of the fossil fuel CO_2 [2]. The concentrations are related by

$$K' = \frac{[HCO_3^-]^2}{[H_2O][CO_3^=][CO_2]}, \qquad (2-2)$$

where the equilibrium constant, K', is a function of salinity, temperature, and pressure. Dissolved inorganic carbon occurs in the upper ocean in the three reduction states of CO_2, and less than 1% of the total dissolved inorganic carbon, denoted ΣCO_2, is found in dissolved CO_2 gas. Consequently, the concentration of total dissolved inorganic carbon can be approximated as the sum of its two major components

$$[\Sigma CO_2] = [HCO_3^-] + [CO_3^=] \qquad \left[\frac{moles}{kg}\right]. \qquad (2-3)$$

Owing to the buffering mechanism expressed by Equation (2-1), the time for CO_2 in surface water to equilibrate with the atmosphere is about 10 times longer than for other gases—to change pCO_2, it is also necessary to change the much larger inventories of $CO_3^=$ and HCO_3^-. Broecker and Peng [2] estimate the step response time of pCO_2 and ΣCO_2 in surface water as about one year.

Reflecting the important role of the negative ions $CO_3^=$ and HCO_3^- in the balance of electrical charge in the sea, alkalinity is defined as the excess of positive charges to be balanced by these ions

$$[Alk] = [HCO_3^-] + 2[CO_3^=] \qquad \left[\frac{moles}{kg}\right]. \qquad (2-4)$$

Therefore, alkalinity is also the sum of the concentrations of positive charges less the concentrations of the remaining negative ions.

Because the activity of water is identically one, Equations (2-2), (2-3), and (2-4) can be manipulated to give the concentration of carbon dioxide gas in terms of the concentration of ΣCO_2, alkalinity, and K'

$$[CO_2] = \frac{1}{K'} \frac{(2[\Sigma CO_2] - [Alk])^2}{[Alk] - [\Sigma CO_2]} \qquad \left[\frac{moles}{kg}\right]. \qquad (2-5)$$

Consequently, one method of determining $[CO_2]$ is to measure $[\Sigma CO_2]$ and $[Alk]$, and use the known dependence of K' on salinity, temperature, and pressure. (The concentration can be converted to mass units using 44.01 g for the molecular weight of CO_2. For example, a concentration of 1 μmole CO_2 per kilogram of seawater corresponds to 0.044 mg CO_2 per kilogram of seawater.)

In air, the partial pressure of CO_2 is the total pressure of the air times the mole fraction of CO_2 in the gas mixture. In water, pCO_2 is the partial pressure of CO_2 in air that is in equilibrium with the solution at the in-situ temperature and pressure. Thus, the CO_2 concentration, $[CO_2]$, is related to the partial pressure, pCO_2, by

$$pCO_2 = \frac{[CO_2]}{\alpha} \qquad [atm], \qquad (2-6)$$

4

where α is the solubility of CO_2 in water, with units of moles CO_2 per kilogram atmosphere. Combining with Equation (2-5),

$$pCO_2 = \frac{1}{\alpha K'} \frac{(2[\Sigma CO_2] - [Alk])^2}{[Alk] - [\Sigma CO_2]} \quad [atm]. \qquad (2-7)$$

As seen in Figure 1, over the range of sea surface temperatures, α decreases by about a factor of two with increasing temperature. (Weiss [23] gives α in terms of fugacity; Heimann and Monfray [8] express Weiss's results in terms of partial pressure.) Owing to the temperature dependence of both α and K', their product varies by a factor of 3.7 between $0°C$ and $30°C$ (Figure 2). As a result, the equilibrium partial pressure increases with increasing temperature by 4%/°C when total carbon and alkalinity are constant. Because the difference in partial pressures between air and water is often only a few percent, the temperature dependence of $\alpha K'$ greatly complicates estimates of the global rate of CO_2 exchange.

Ray Weiss, at Scripps Institution of Oceanography, measures ΔpCO_2 by drawing samples of air and water while a ship is underway. The partial pressure of the ocean, $(pCO_2)_{oce}$, is determined by equilibrating the water and air samples at the in-situ temperature and pressure. The samples are then dried and analyzed in a gas chromatograph, and the results are reported in terms of x_{CO_2}, the moles of CO_2 per mole of dry air. Examples are shown in Figures 3 and 4. Conversion of x_{CO_2} requires knowledge of the humidity expressed as the partial pressure of water, p_{H_2O}, in terms of which

$$pCO_2 = (P_{total} - p_{H_2O})x_{CO_2} \quad [atm], \qquad (2-8)$$

where P_{total} is the total pressure (this is equation 10 of Weiss and Price [25]). To determine the average flux, it would be appropriate to use the average

5
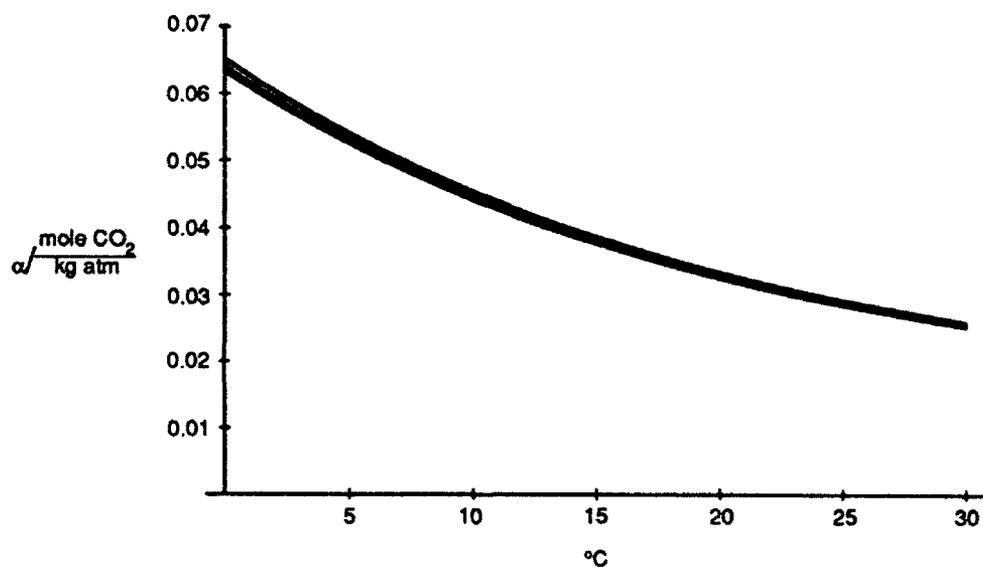
Figure 1. Solubility of CO_2 in seawater [Reference 23]. Plotted for salinities of 32, 35, and 37 psu, the variability with salinity is much less than with temperature.

6
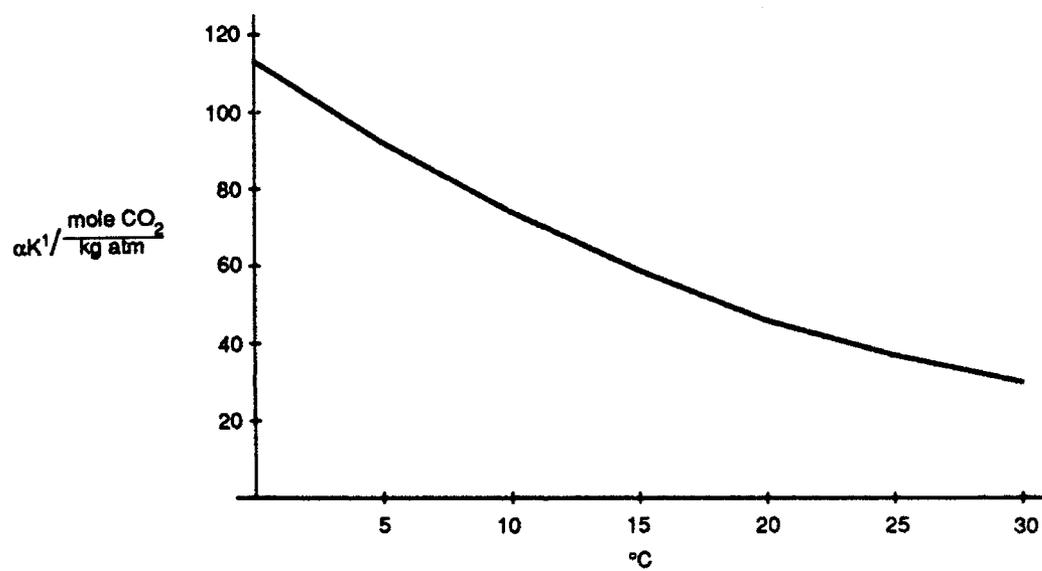
Figure 2. The product of the solubility, α, and the equilibrium constant, K' for CO_2 in seawater, based on data in Table 3.7 [Reference 2]. The product decreases by a factor of 3.7 as water warms from 0°C to 30°C.
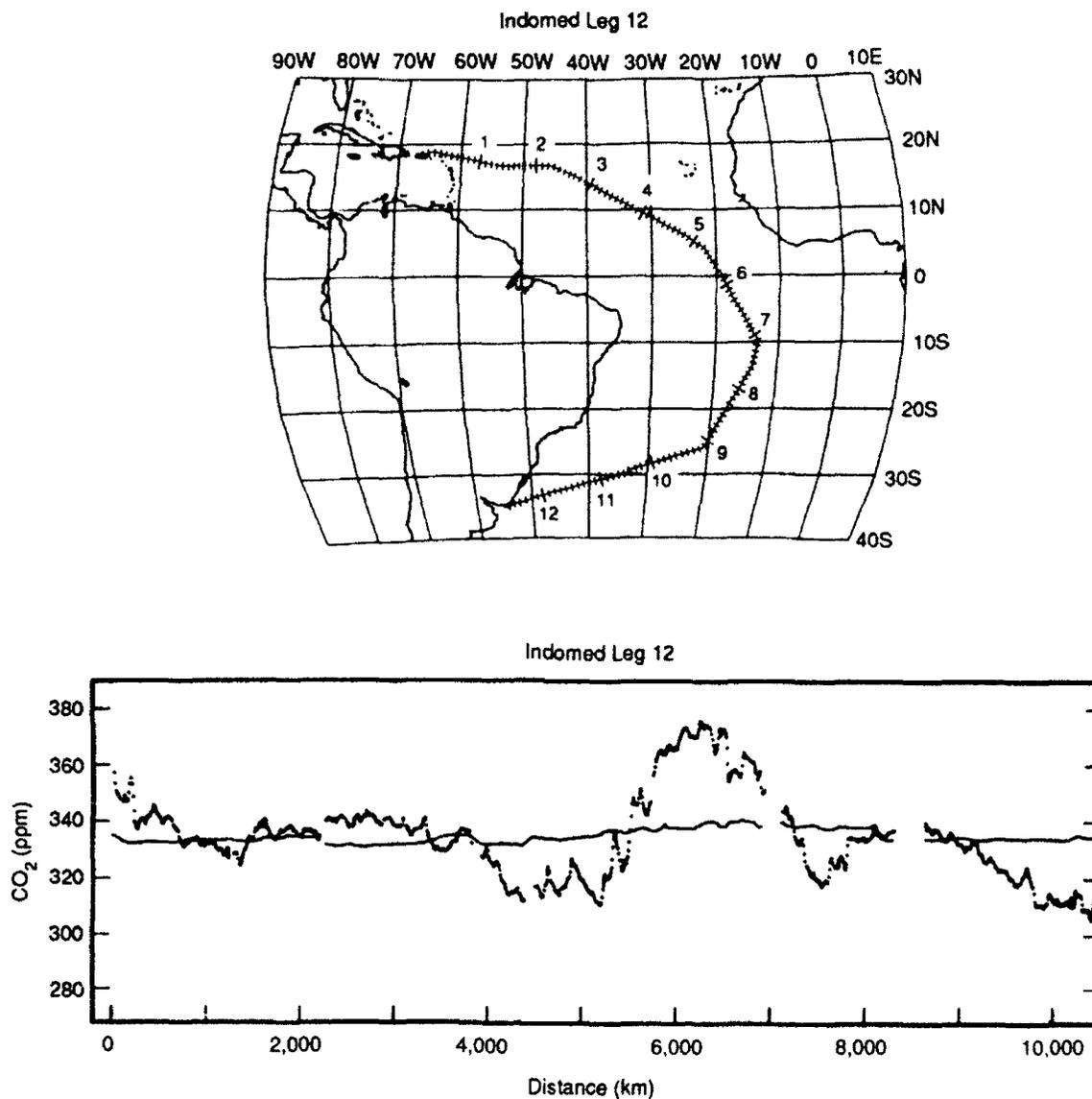
Figure 3. Mole fractions of CO_2 in air and water measured continously during Leg 12 of the INDOMED cruise from Puerto Rico to Buenos Aires from 21 September to 1 November 1978 [Reference 24]. As the differences in mole fractions are close to differences in partial pressures, the large excess of XCO_2 in the water near the equator reflects strong outgassing up the upwelling water.
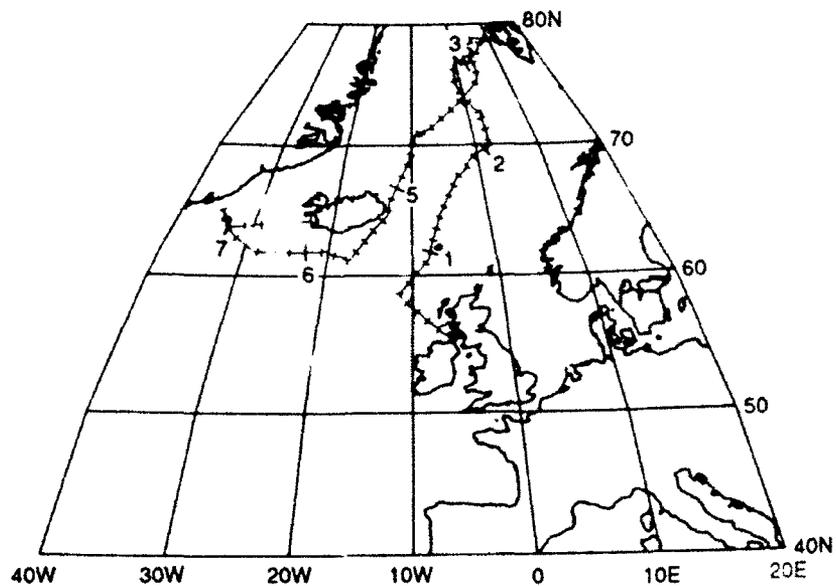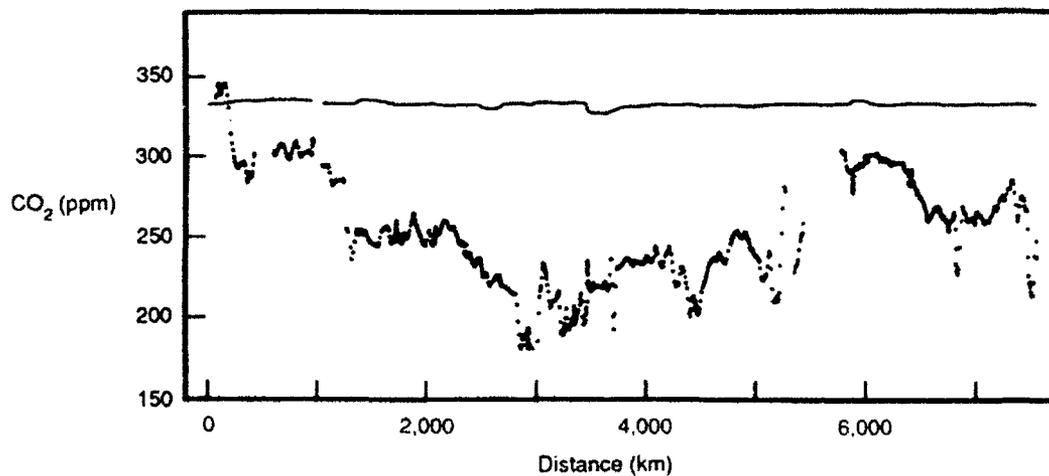
Figure 4. Mole fractions of CO_2 in air and water measured continously during Leg 5 of the North Atlantic Study of the Transient Tracers cruise from Glasgow to Revjavik between 19 June and 15 July 1981 [Reference 24]. The large deficit of XCO_2 reflects strong absorption in the North Atlantic at high latitudes.

9

$(p_{H_2O})_{air}$, since x_{CO_2} is relatively constant over time. As evident in Figure 5, the correction for p_{H_2O} is small, but it greatly increases with temperature.

Biology is also an important aspect of the carbon chemistry of the sea and one that is likely to be strongly correlated with wind speed. Deepening surface mixed layers often entrain nutrient-rich waters from the thermocline, producing an explosive growth of phytoplankton in the mixed layer. These issues are beyond the scope of this preliminary survey, but are important and need careful study.
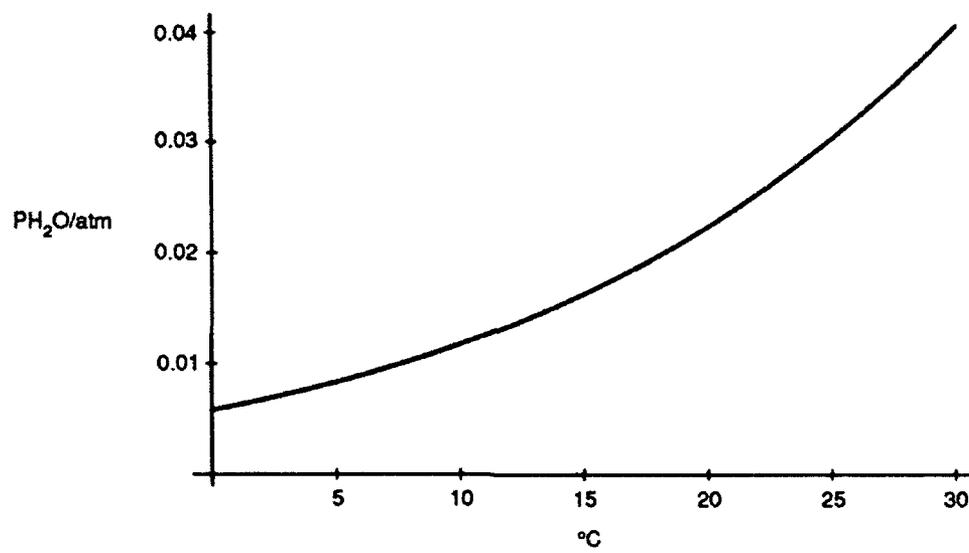
Figure 5. The partial pressure of water vapor in air is a small correction, but increases strongly with temperature [Reference 25].

3 BULK FLUXES

The bulk flux is formulated as

$$F_{CO_2} = E \cdot [(pCO_2)_{atm} - (pCO_2)_{oce}] \qquad (3\text{-}1)$$

$$= E \cdot \Delta pCO_2 \qquad [\text{mol } CO_2 \text{ m}^{-2} \text{ s}^{-1}], \qquad (3\text{-}2)$$

where E is the gas exchange coefficient with units of moles CO_2 m^{-2} s^{-1} atm^{-1}, and ΔpCO_2 is in atm.

The atmosphere is well mixed in CO_2, with a mean concentration close to 350 ppm. The principal variability is an annual cycle of about 5 ppm (resulting from the yearly change in plant respiration) and a mean north/south gradient of about 3 ppm (resulting from greater release of fossil fuel in the northern hemisphere). In surface waters, oceanic concentrations range from 150 to 450 ppm. Therefore, changes in the driving potential for CO_2 exchange across the sea surface result largely from changes of $(pCO_2)_{oce}$.

The partial pressure of CO_2 in the surface water is measured by two methods. One, described earlier, is Weiss's which uses an air/water equilibrator connected to a gas chromotograph. This approach operates continuously while the ship is underway and determines $(pCO_2)_{atm}$ and $(pCO_2)_{oce}$. The other method, used by Taro Takahashi at Lamont, is to collect bulk water samples, determine the total carbon and pCO_2 at a standard temperature, and then correct pCO_2 to in-situ values using the temperature dependences of the solubility and the equilibrium constants. Comparisons of simultaneous measurements reveal root mean square (rms) differences of 6-7 μatm between

13

the two techniques, and along some ship tracks biases of 2-3 μatm have been found [24]. Although these errors are relatively small compared to the concentration of CO_2, they sometimes exceed the *difference* in concentration between air and water over large areas of the ocean. For the first 4,000 km of Weiss's measurements from San Juan to Buenos Aires (Figure 3), the difference in concentrations of CO_2 between air and water is no more than 10 ppm and changes sign several times. In other locations the errors will indeed be small relative to the contrast in partial pressures. For instance, upwelling produces a large excess of CO_2 in the surface water at the equator causing outgassing. Another case of large contrasts occurs at high latitudes during summer in the North Altantic (Figure 4). For several thousand kilometers, the oceanic concentration is about 130 ppm less than the atmospheric value causing strong absorption.

The gas exchange coefficient is usually expressed as

$$E = \alpha \, V_{\mathrm{p}} \qquad [\text{moles } CO_2 \text{ m}^{-2} \text{ s}^{-1}], \qquad (3-3)$$

with V_{p} as the gas-exhange velocity. Also known as the piston velocity, V_{p} is not well known. Presently, the most realistic parameterization [11] expresses it in terms of temperature and wind speed

$$V_{\mathrm{p}} = \begin{cases} \left(\frac{Sc(T)}{600}\right)^{-2/3} 4.7 \times 10^{-7} U_{10} & U_{10} \leq 3.6 \\ \left(\frac{Sc(T)}{600}\right)^{-1/2} (7.92 \times 10^{-6} U_{10} - 2.68 \times 10^{-5}) & 3.6 < U_{10} \leq 13 \\ \left(\frac{Sc(T)}{600}\right)^{-1/2} (1.64 \times 10^{-5} U_{10} - 1.369 \times 10^{-4}) & 13 < U_{10} \end{cases}$$

$$(3-4)$$

where V_{p} is in m/s, U_{10} is the wind speed (in m/s) at 10 m above the sea surface, and Sc is the Schmitt number for CO_2 in water.

The temperature dependence occurs via the Schmitt number, defined

as the ratio of the kinematic viscosity, ν, to the diffusivity of CO_2 in water, κ_{CO_2}, both of which vary with temperature. As $\nu \approx 1 \times 10^{-6}$ m^2 s^{-1} and $\kappa_{CO_2} = 1$ to 2×10^{-9} m^2 s^{-1}, $Sc \approx 600$ at 20°C. Between 0°C and 30°C, $Sc/600$ varies more than a factor of three, decreasing with increasing temperature. (Sc also varies with salinity, but the effect is slight and can be ignored for CO_2 studies.) Owing to this dependence of Sc, V_p increases with temperature by about a factor of two (Figure 6).

This increase of V_p, however, is offset by the decrease of the solubility, α. As a result, the CO_2 exchange coefficient, E, varies little with temperature (Figure 7).

Liss and Merlivat [11] proposed the wind speed dependence in Equation (3-4) based on an approximate fit to measurements in wind tunnels and over lakes. The increase of V_p with wind speed (Figure 8) differs from the transfer coefficients for heat, water vapor, and momentum, which show little change with U_{10} when the atmosphere is weakly stratified. Transfer coefficients for other quantities increase nearly linearly with U_{10}, but gases seem to have a stronger dependence. This is not surprising since the molecular diffusivity κ_{CO_2} is very small, resulting in a resistance to transport almost entirely from the water phase.

Bubbles may play an important role in gas transfer for two reasons. First, bubbles greatly increase the total area of the air-sea interface. Because the resistance to transport is so completely in the water, bubbles lasting longer than turbulent eddies in the air can still be important to gas transfer. Second, the global average of ΔpCO_2 is of the order of 10 μatm, much smaller

15
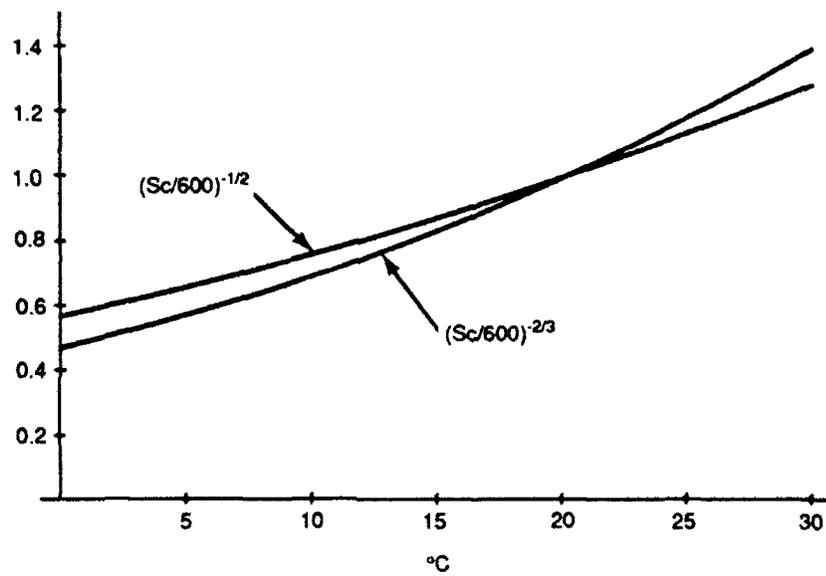
Figure 6. Temperature dependence of the piston velocity, where $Sc = 10^{(-3.889 + 1955/T)}$ [Reference 8] based on data in [Reference 7].
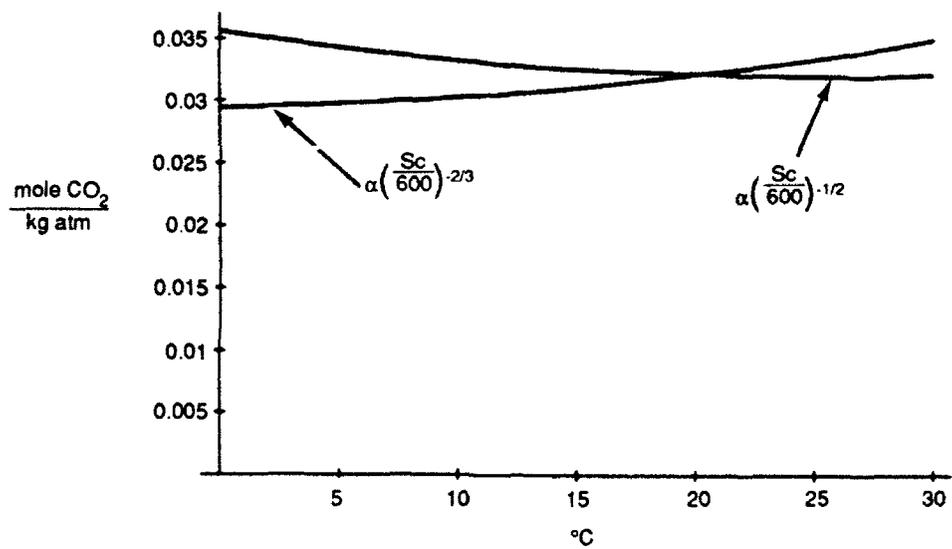
Figure 7. Total temperature dependence of the exchange velocity, E, varies little with temperature, owing to compensating effects in the solubility, *alpha*, and in the Schmitt number dependence of the piston velocity.
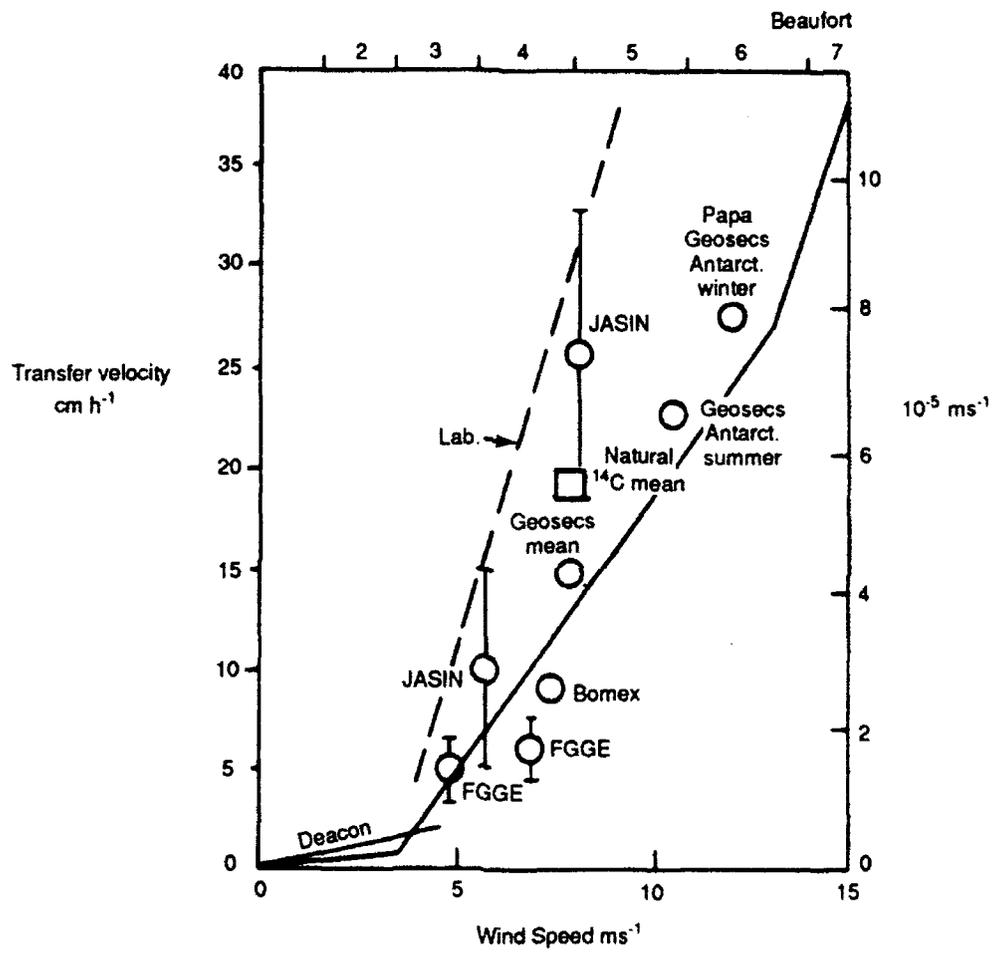
Figure 8. Variation of the piston velocity V_p, with wind speed (solid) compared with observations and other models [Reference 11].

than $(pCO_2)_{atm}$, which is approximately 350 μatm. Small bubbles are routinely observed several meters below the surface [5] and their concentration increases rapidly with U_{10}, perhaps as U_{10}^3. Owing to surface tension, the pressure inside small bubbles is higher than the hydrostatic pressure. Thus, the effect of bubbles on gas transfer, discussed by Thorpe [22], could cause E to vary rapidly with wind speed. In a similar way, small ripples which modulate the thin diffusive boundary layer below the air-sea interface may be important for gas transfer. Because much of the information about the piston velocity comes from laboratory wind tunnels, it is not clear how well these measurements reflect gas transfer in a fully developed wind-driven sea.

Owing to the non-linear dependence of E on U_{10}, instantaneous wind speeds are essential for evaluating Equation (3-4). Laboratory and local oceanic field studies of gas transfer are based on instantaneous winds, and the non-linear dependence does not permit the use of temporally or spatially averaged winds. As a minimum, reasonably accurate probability density functions should be used to calculate the average exchange coefficient, $< E >$.

4 TURBULENT FLUXES

Carbon dioxide fluxes are obtained directly in the atmospheric boundary layer by measuring the correlation between fluctuations in vertical velocity and fluctuations in the CO_2 concentration

$$F_{CO_2} = a\, \overline{w'c'} \qquad [\text{mg } CO_2 \text{ m}^{-2} \text{ s}^{-1}], \qquad (4-1)$$

where w' is in m/s, and c' is in mg CO_2/m^3. Turbulence investigators express F_{CO_2} in units of mg CO_2/m^2 s, in which case $a = 1$. The molecular weight of CO_2 is used to convert to geochemical units, i.e., $a = (1/44 \times 10^3$ mg per mole CO_2). Some geochemists use units of mole CO_2 m^{-2} year^{-1} [3]. These can be converted to the units of the turbulence investigators using 1 mole CO_2 m^{-2} year^{-1} = 1.40×10^{-3} mg CO_2 m^{-2} s^{-1}. Similarly, CO_2 concentrations can be converted by 1 ppm CO_2 = 1.83 mg CO_2 m^{-3}.

Beginning over a decade ago, turbulence measurements of CO_2 have developed slowly [9], [12], [17], [26] and generated sharp controversy. To the extent that they have been compared, the turbulent results exceed the bulk fluxes by factors of 5 to 10. Rejecting the turbulence fluxes, most of the geochemists attacked [3], pointing out the low signal-to-noise levels of the CO_2 measurements and citing agreement between their fluxes and bulk constraints imposed by: 1) distributions of naturally occurring ^{14}C between ocean and atmosphere, 2) evasion rates of radon from surface waters, and 3) global distributions of bomb [14]C. Smith and Jones [18] and Wesley [27] defended their measurements.

Carbon dioxide fluxes are very low over the ocean compared to those over land, where growing crops produce fluxes of 1 to 2 mg CO_2/m^2 s ($2\text{-}4 \times 10^{-5}$ moles CO_2/m^2 s), values which match the fluxes predicted by agricultural measurements. By contrast, 0.083 mg CO_2/m^2 s was the largest magnitude observed by Smith et al. [19]. With such weak fluxes, noise and drift are key issues for evaluating fluxes over water.

The turbulence measurements are made with two sensors located within approximately 1 m of each other. Sonic anemometers detect w' and infrared absorption detectors sense CO_2. The new generation of sensors detects the absorption from a strong infrared source (at a temperature of about 1,000 K) over a path in the air of 0.2 to 0.25 m. Attenuation is compared between a wavelength of 4.3 μm, center of the strong CO_2 absorption bands, and 3.9 μm, which is not absorbed. To remove the effects of absorption by water vapor, attenuation is also compared between 2.6 μm, center of the water vapor absorption bands, and 3.9 μm. Smith et al. report peak-to-peak noise of 0.3 mg CO_2/m^3, a factor of ten lower than for their previous measurements.

The new sensors reveal the same discrepancy with the bulk formulas as before. For $U_{10} = 3$ to 9 m/s Smith et al. [19] report

$$V_p = 6.5 \times 10^{-5} \, U_{10} \qquad \text{[m/s]}. \qquad (4-2)$$

Comparison with the bulk formulas shows that the direct measurements are larger by factors of 5 to 10 (Figure 9). Furthermore, cospectra of w' and c' are very similar to those of w' and T' and of w' and q', where q' is the fluctuation in water vapor (Figure 10).
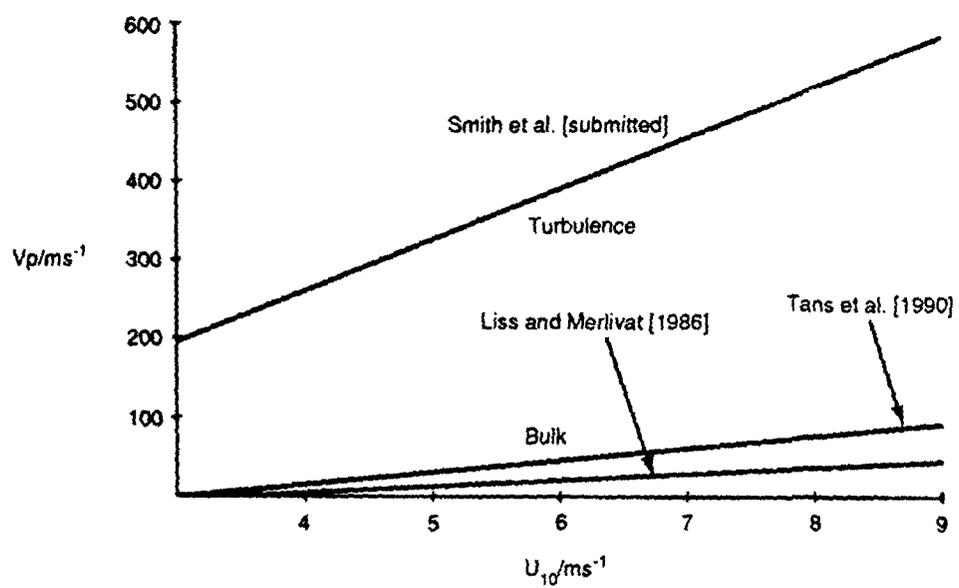
Figure 9. The piston velocity obtained from direct turbulent measurements by [Reference 19] is 5 to 10 times larger than that given at the same wind speed by bulk formulas. The comparison is plotted only over the range of U_{10} observed by Smith et al.
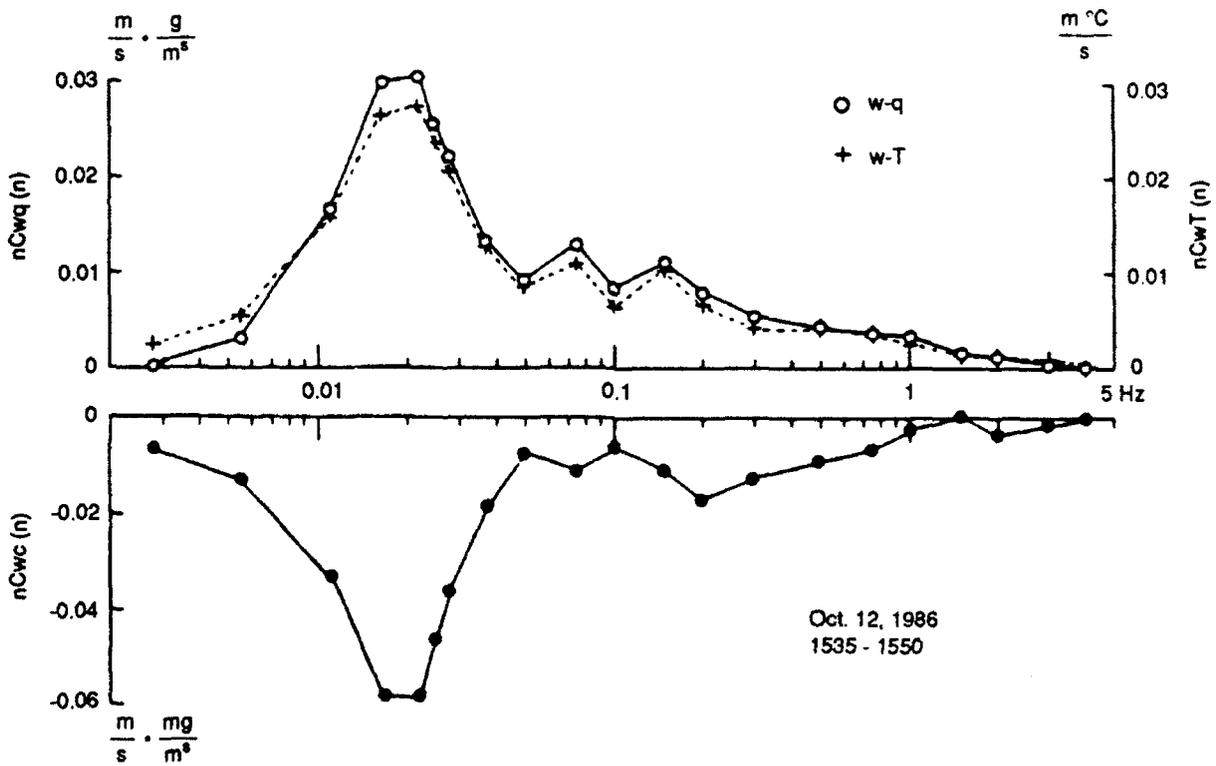
Figure 10. Cospectra of w' with (1) CO_2 concentration (solid circles), (2) temperature (open circles), and (3) water vapor (+) [Reference 13]. The structure of the cospectrum with CO_2 is very similar to that of the other variables.

24

We conclude that the turbulent measurements seem as carefully done as those for other atmospheric variables and cannot be dismissed. Neither, however, can we dismiss the bulk constraints cited by the geochemists as justification that the bulk formulas give the correct magnitude for average fluxes over large areas. The discrepancy probably results from differences in the space and time scales of the two approaches, as argued by Smith and Jones [18]. Nevertheless, the controversy needs to be resolved soon.

5 MEASURING WINDS

It is tempting to compute time and space averages of CO_2 exchange from the average wind speed, and this is frequently done. For example, Tans et al. [21] use a linear dependence on wind speed

$$E = \begin{cases} 0 & U_{10} < 0 \\ 0.016(U_{10} - 3) & 3 \le U_{10} \end{cases} \quad \left[\frac{\text{moles } CO_2}{\text{m}^2 \text{ year } \mu\text{atm}} \right], \quad (5-1)$$

which they attribute to Peng and Takahashi [14]. To compensate for the linear dependence, this expression doubles V_p relative to the Liss and Merlivat formulation. If V_p and E varied linearly with wind speed (as they do for heat transfer), this would be acceptable so long as ΔpCO_2 fluctuations were constant or varied with wind variations. But, as the empirical law in Equation (3-4) indicates, the relation between transfer rate and wind speed is nonlinear. It is, therefore, unacceptable to replace the average of E with E evaluated at the average wind speed, i.e., to replace $< E(U_{10}) >$ with $E(< U_{10} >)$. As a minimum, a reasonably accurate probability density of wind speed is required to calculate an average exchange coefficient. Beyond this, the covariation of ΔpCO_2 and wind speed could be deduced and used for better estimates of average fluxes.

Direct observations of wind speed from oceanographic buoys are sufficiently accurate for estimating fluxes, but buoys are too scarce to be of much help for global distributions. Routine ship observations are much more numerous. Many are based on visual identification of the sea state, which represents an average of an hour or so, owing to the finite growth rate of the

27

short waves most affecting the appearance of the sea. Because the observers are frequently well trained, these data are consistent and useful [16], so much so that scatter between such wind estimates is about 25% and averages from different observers agree to about 10% [20]. Well-placed ship anemometers with good exposure appear to agree with buoy observations to 5%, but the same ship on a different course relative to the wind may yield errors of 30%. The main problem with direct observations, however, is their low density, particularly in the southern hemisphere and in high latitudes during winter. Efforts are underway to improve the ability of operational weather forecasting models to estimate the wind information needed for flux estimates, but success has not been demonstrated where data are sparse.

Can adequate winds be determined from satellites? Essentially three types of satellite sensors can be used to estimate wind speeds. Radar scatterometers are designed to measure wind speed and direction. Comparisons of the Seasat scatterometer with direct wind observations from oceanographic buoys indicate a scatter of about ±2 m/s for speeds of 0 to 12 m/s. Using the same phenomenon, i.e., increasing surface roughness with wind speed, radar altimeters measure wind speed (but not direction). Because of the vertical angle of incidence, these measurements should be slightly less accurate than those from a scatterometer, but Chelton and McCabe [4] find the degradation to be slight. Finally, passive microwave sensors also respond to wind speed variations, presumably because wind-generated surface roughness affects the microwave emissivity. Comparison of winds derived from the SMMR radiometer on Seasat with winds from buoys showed a scatter as little as ±1 m/s [1].

Both direct and satellite wind observations have instrumental errors and potential biases. Nevertheless, by comparing Seasat winds with direct observations and analyzed field reports, Chelton [private communication] finds that the largest errors in wind statistics come from inadequate sampling. Even though a satellite makes many more observations than all the ships at sea, the influence of unobserved wind events on the climatology is still the greatest source of error. Thus, the best estimates of wind climatologies would be obtained by combining all satellite sensors with all avaliable direct observations.

No scatterometers are presently operating, but the European satellite ERS-1, launched in mid-1991, will have a part-time scatterometer. An identical satellite, ERS-2, is scheduled for 1994. The U.S. and Japanese NSCAT/ADEOS scatterometer will be more accurate, and it will sample continuously. It is scheduled for 1995. The ERS satellites will both carry altimeters, which could yield wind data, and the TOPEX/POSEIDON altimeter is scheduled for mid-1992. The SMM/I passive microwave radiometer carried aboard operational Air Force DMSP satellites is now available for estimating wind speeds, and this series is likely to be extended in the future. Thus, there will be a number of wind-sensing satellites available in the next decade which, with a significant effort, could be combined to provide oceanic wind fields of greater accuracy than available now.

6 CONCLUSIONS AND RECOMMENDA-TIONS

6.1 Conclusions

Direct flux measurements are necessary for developing correct bulk parameterizations, but they are far too restricted in space and time for estimating global average CO_2 fluxes. Only bulk formulas are practical for estimating space and time averages as $< F_{CO_2} >=< E \cdot \Delta pCO_2 >$. In our cursory review of the CO_2 flux problem, we find important uncertainities about: 1) the adequacy of ΔpCO_2 sampling and whether the data are sufficient for computing accurate averages, 2) the dependence of E on wind speed and temperature, 3) the adequacy of climatological winds and average ΔpCO_2 for computing average fluxes, and 4) the chemical procedures for calculating ΔpCO_2. In view of these uncertainities, calculations of net fluxes are certain to disagree so wildly that we conclude it is not known how to compute the present air-to-ocean flux or to predict future changes. Because predicting future CO_2 concentrations in the atmosphere is the first step in assessing global warming and because transport of CO_2 to the ocean is comparable with the rate of accumulation of CO_2, we perceive an urgent need to resolve these uncertainities about the air-sea CO_2 flux.

Both ΔpCO_2 and E (which depends primarily on wind speed) vary substantially in time and space. Although extensive measurements of ΔpCO_2 have been made, they are a small fraction of the number of wind speed mea-

surements. Furthermore, only a small fraction of the collected data have been published, leading to uncertainities about the quality and coverage of ΔpCO_2 data used in calculations. Owing to variations of CO_2 concentration, temperature, alkalinity, and total dissolved carbon dioxide, ΔpCO_2 varies substantially in space (see Figures 3 and 4) and in time. Because the global average of ΔpCO_2 is only a few ppm (see Figure 8 which shows zonal averages) and much less than its variability, accurate space and time averages are essential.

Few repeated observations exist for determining time variability in pCO_2, or perhaps more importantly, for determining the factors causing the variability. Wong et al. [28] and collaborators reportedly have analyzed data from Ocean Weather Station P, in the Gulf of Alaska, and found that random variability makes it impossible to detect a seasonal cycle or determine an accurate mean value. If this is generally true, a time average can certainly not be computed from two or three samples. Figures 3 and 4 show that ΔpCO_2 is subject to rapid, front-like variations which are several times larger than the differences in the zonal averages shown in Figure 11. Consequently, high spatial resolution will be required for accurate spatial averages. At the very least, diligent study is needed to define the sampling needed for realistic space-time averages.

Figure 12 shows the ship tracks used by Tans et al. [21]. Since many of the data were obtained from commercial ships following trade routes, coverage is good in northern temperate latitudes, particularly in the North Atlantic. Winter observations in high latitudes are rare, even in the North
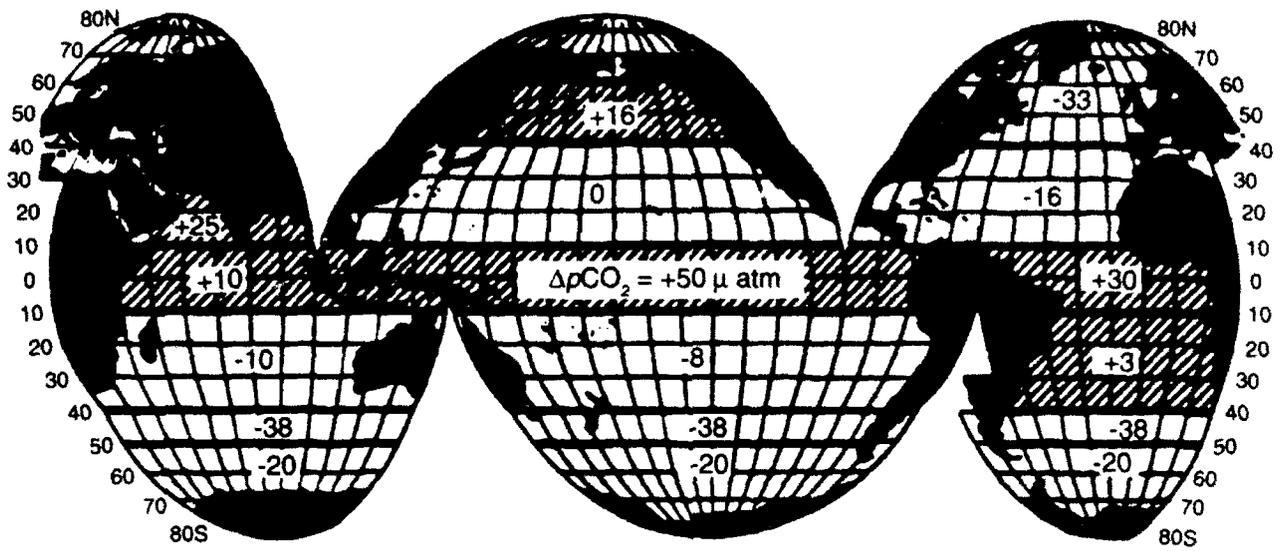
Figure 11. Zonal averages of ΔpCO_2 reported by [Reference 3].

Figure 12. Ship tracks along which ΔpCO_2 data used by [Reference 21] were collected. Compare the density of tracks along shipping routes in the North and South Pacific with the Southern Ocean in the Pacific and Indian sectors.

Pacific, but especially in the Southern Ocean, where very large fluxes are expected in winter. Figure 3 from Tans et al. reveals no data at all in the Pacific and Indian Ocean sectors of the Southern Ocean during austral winter. With data gaps of this magnitude, it is hard to take the results of Tans et al. seriously.

Although the Liss and Merlivat [11] parameterization for V_p seems to be the most realistic at present, the measurements on which it is based come mainly from laboratory wind tunnels and are unlikely to represent oceanic conditions where fluxes are expected to be largest. This parameterization should be viewed as a promising beginning rather than as a definitive result.

Tans et al. [21] estimated the global mean flux, $< F_{CO_2} >=< E(U_{10}) \cdot \Delta p CO_2 >$ by multiplying averages of the mean wind speeds and mean $\Delta p CO_2$, i.e., they computed $< F_{CO_2} > = E(< U_{10} >) \cdot < \Delta p CO_2 >$. The V_p algorithm of Liss and Merlivat [11] shows that E increases nonlinearly with wind speed. Consequently, as shown by Etcheto and Merlivat [6] using climatological winds is inadequate. If $\Delta p CO_2$ were constant or varied independently from U_{10}, then it would follow that $< F_{CO_2} = E(< U_{10} >) \cdot < \Delta p CO_2 >$ and $< E >$ could be computed from the probability density of U_{10}, or possibly from climatological winds by applying corrections based on typical fluctuations. But Tans et al. did not account for fluctuations and, indeed, in footnote 23 they state that using instantaneous winds with V_p from Liss and Merlivat would increase absorption by 25% in the Northern hemisphere and 50% in the Southern Ocean.

While independence of $\Delta p CO_2$ and U_{10} fluctuations would simplify de-

termination of the average flux, there are two competing reasons why there may be a correlation of these fluctuations. First, because CO_2 solubility depends on temperature, $(pCO_2)_{oce}$ has a strong temperature dependence, even if the concentration $[CO_2]$ remains constant. Strong winds deepen the mixed layer, entraining cold water into it. The resulting correlation of ΔpCO_2 and U_{10} tends to increase fluxes into the ocean over what would be found without such correlation. At the same time, entrainment typically increases $[CO_2]$ in the mixed layer, owing to higher concentrations of CO_2 in the deeper water. Since cooling by 1°C can lower $(pCO_2)_{oce}$ about 10 ppm, it is quite possible for these effects to change the sign of the mean flux as well as its magnitude. For example, Figure 8 shows $\Delta pCO_2 \approx 0$ over much of the North Pacific, so that accounting for a correlation between ΔpCO_2 and U_{10} may significantly change the computed flux. Finally, wind-driven entrainment also brings nutrients into the mixed layer, leading to the possibility that biological activity may also cause additional correlation of ΔpCO_2 and wind speed.

Because the global mean ΔpCO_2 is so small, it is critical that the chemical procedures used to measure it be accurate to a very few ppm. Although a sample-to-sample noise several times larger would little affect the averages, it is critical that there not be a mean bias error. We are unaware of successful comparisons of different methods to show that consistent measurements can be made.

36

6.2 Recommendations

In view of the wide disparity in the algorithms and in the data used for computing CO_2 fluxes, little can be expected from further calculations until better algorithms are developed and the data improved. Several steps are needed.

1. A program should be established to determine V_p at sea, as is done for transfer coefficients for momentum, heat, and moisture. This will require extensive measurements by geochemists and turbulence investigators working at the same place and time from platforms and ships. After rationalizing bulk and turbulent fluxes at low and moderate wind speeds, the measurements should be extended to the high winds producing the high φ s transfer rates in the Southern Ocean.

2. The observational work to determine V_p should be coupled with measurements of wave breaking and subsurface bubbles and with theoretical and laboratory work on the role of bubbles in gas transfer.

3. Investigators measuring CO_2 at sea should be funded to publish their observations, and they should be encouraged to adopt common methods of measurement, with suitable controls. A standard is needed before beginning systemmatic sampling of ΔpCO_2.

4. Systemmatic observations should be established to obtain adequate global and seasonal coverage of pCO_2. At present observations are constrained to piggyback on ship tracks established for other purposes, leading to relatively dense sampling of the North Atlantic and sparse

sampling of the Southern Ocean. Owing to the fundamental importance of CO_2 to the assessment of global warming, the measurement program should seek adequate coverage within 10 to 15 years.

5. Time series stations should be established to determine the time variability of ΔpCO_2 and its causes. The observations should include mixed layer parameters to test whether entrainment causes ΔpCO_2 to vary and whether the variation can be parameterized in terms of wind speed. Biological parameters should also be monitored to assess the importance of biological productivity. Similar studies may be needed in several oceanographic and biological regimes. This observational program should lead a vigorous theoretical program to interpret the observed variations and model mean fluxes more accurately than by combining mean ΔpCO_2 fields and mean winds.

6. The observational base of ΔpCO_2 should be expanded and a concerted effort should be made to obtain all available wind observations so that the global average flux can credible estimated. Analysis of time series and repeated sections should be used to estimate the sampling errors associated with different sampling strategies and to select efficient ones.

References

[1] Allan, T. D. and T. H. Guymer (1984), Seasat measurements of wind and waves on selected passes over JASIN, *Int. J. Rem. Sens.*, **5**, 379–408.

[2] Broecker, W. S. and T.-H. Peng (1982), *Tracers in the Sea*, Lamont-Doherty Geological Observatory, Palisades, N.Y., 690.

[3] Broecker, W. S., J. R. Ledwell, T. Takahashi, R. Weiss, L. Merlivat, L. Memery, T.-H. Peng, B. Jähne, and K. O. Munnich (1986), Isotropic versus micrometerologic ocean CO_2 fluxes: A serious conflict, *J. Geophys. Res.*, **91**, 10,517–10,527.

[4] Chelton, D. B. and P. J. McCabe (1985), A review of satellite altimeter measurement of sea surface wind speed: with a proposed new algorithm, *J. Geophys. Res.*, **90**, 4707–4720.

[5] Crawford, G. B. and D. M. Farmer (1987), On the spatial distribution of bubble clouds, *J. Geophys. Res.*, **92**, 8231–8242.

[6] Etcheto, J. and L. Merlivat (1988), Satellite determination of the carbon dioxide exchange coefficient at the ocean–atmosphere interface: A first step, *J. Geophys. Res.*, **93**, 15,669–15,678.

[7] Jähne, B., G. Heinz, and W. Dietrich (1987), Measurement of the diffusion coefficients of sparingly soluble gases in water, *J. Geophys. Res.*, **92**, 10,767–10,776.

[8] Heimann, M. and P. Monfray (1989), Spatial and temporal variation of the gas exchange coefficient for CO_2: 1. Data analysis and global validation, Report 31 of the Max-Planck-Institut für Meteorologie, Hamburg.

[9] Jones, E. P. and S. D. Smith (1977), A first measurement of sea-air CO_2 flux by eddy correlation, *J. Geophys. Res.*, **82**, 5990–5992.

[10] Levine, J. S. (1990), Global biomass burning: atmospheric, climatic and biospheric implications, *Eos*, **71**, 1075–1077.

[11] Liss, P. S. and L. Merlivat (1986), Air-sea gas exchange rates: An introduction and synthesis, *The Role of Air-Sea Exchange in Geochemical Cycling*, P. Buat-Mènard (ed.), *Adv. Sci. Inst. Ser. 185*, D. Reidel, 113–127.

[12] Ohtaki, E. (1984), Application of an infrared carbon dioxide and humidity instrument to studies of turbulent transport, *Boundary-Layer Meteorology*, **29**, 85–107.

[13] Ohatki, E., O. Tsukamoto, Y. Iwatani, and Y. Mitsuta (1989), Measurements of the carbon dioxide flux over the ocean, *J. Meteor. Soc. Japan*, **67**, 541–554.

[14] Peng, T.-H. and T. Takahashi, in *Biogeochemistry of* CO_2 *and the Greenhouse effect*, P. Farrell, (ed.) *Am. Chem. Soc. Symp.*, CRC/Lewis, Boca Raton, FL, in press.

[15] Revelle, R. and H. E. Suess (1957), Carbon dioxide exchange between atmosphere and ocean and the question of an increase of atmospheric CO_2 during the past decades, *Tellus*, **9**, 18–27.

[16] Shearman, R. J. (1983), The Meteorological Office main marine data bank, *Marine Observer, London*.

[17] Smith, S. D. and E. P. Jones (1985), Evidence for wind-pumping of air-sea gas exchange based on direct measurements of CO_2 fluxes, *J. Geophys. Res.*, **90**, 869–875.

[18] Smith, S. D. and E. P. Jones (1986), Isotopic and micrometeorological ocean CO_2 fluxes: Different time and space scales, *J. Geophys. Res.*, **91**, 10,529–10,535.

[19] Smith, S. D., R. J. Anderson, E. P. Jones, R. L. Desjardins, R. M. Moore, O. Hertzman, and B. D. Johnson, A new measurement of CO_2 eddy flux in the marine atmospheric surface layer, *J. Geophys. Res.*, submitted.

[20] Taylor, P. K. (1984), The determination of surface fluxes of heat and water by satellite microwave radiometry and *in situ* measurements, in

Large Scale Oceanographic Experiments and Satellites, Isotropic by Gautier and Fieux, 223–246.

[21] Tans, P. P., I. Y. Fung, and T. Takahashi (1990), Observational constraints on the global atmospheric CO_2 budget, *Science*, 1431–1438.

[22] Thorpe, S. A. (1982), On the clouds of bubbles formed by breaking wind waves in deep water, and their role in air-sea gas transfer, *Phil. Trans. R. Soc. London*, **A304**, 155–210.

[23] Weiss, R. F. (1974), Carbon Dioxide in water and seawater: the solubility of a non-ideal gas, *Marine Chemistry*, **2**, 203–215.

[24] Weiss, R. F. (1990), *Surface Water and Atmospheric Carbon Dioxide and Nitrous Oxide Observations by Shipboard Automated Gas Chromotography, 1977–1989*, unpublished report.

[25] Weiss, R. F. and B. A. Price (1980), Nitrous oxide solubility in water and seawater, *Marine Chemistry*, **8**, 347–359.

[26] Wesley, M. L., D. R. Cook, R. L. Hart, and R. M. Williams (1982), Air-sea exchange of CO_2 and evidence for enhanced upward fluxes, *J. Geophys. Res.*, **87**, 8827–8832.

[27] Wesley, M. L. (1986), Response to "Isotopic versus micrometerologic ocean CO_2 fluxes: A serious conflict," by Broecker et al., *J. Geophys. Res.*, **91**, 10,533–10,535.

[28] Wong, C. S., R. D. Bellegay, G. E. Smith, J. S. Page, and Y.-H. Chan (1985), Seasonal changes in pCO_2 in surface Pacific Ocean. *Atmospheric carbon dioxide, its sources, sinks and global transport*, Proceedings of the Kandersteg Conference, Commission on Atmospheric Chemistry and Global Pollution of the International Association of Meteorology and Atmospheric Physics, 189–196.

DISTRIBUTION LIST

CMDR & Program Executive Officer
U S Army/CSSD-ZA
Strategic Defense Command
PO Box 15280
Arlington, VA 22215-0150

Mr John M Bachkosky
Deputy DDR&E
The Pentagon
Room 3E114
Washington, DC 20301

Dr Joseph Ball
Central Intelligence Agency
Washington, DC 20505

Dr Arthur E Bisson
DASWD (OASN/RD&A)
The Pentagon
Room 5C675
Washington, DC 20350-1000

Dr Albert Brandenstein
Chief Scientist
Office of Nat'l Drug Control Policy
Executive Office of the President
Washington, DC 20500

Mr. Edward Brown
Assistant Director
DARPA/NMRO
3701 North Fairfax Drive
Arlington, VA 22203

Dr H Lee Buchanan, I I I
Director
DARPA/DSO
3701 North Fairfax Drive
Arlington, VA 22203-1714

Dr Curtis G Callan Jr
Physics Department
PO Box 708
Princeton University
Princeton, NJ 08544

Dr Kenneth M Case
1429 Calle Altura
La Jolla, CA 92037

Dr Ferdinand N Cirillo Jr
Central Intelligence Agency
Washington, DC 20505

Ambassador Henry F Cooper
Director/SDIO-D
Room 1E1081
The Pentagon
Washington, DC 20301-7100

D A R P A Library
3701 North Fairfax Drive
Arlington, VA 22209-2308

D T I C [2]
Cameron Station
Alexandria, VA 22314

Mr John Darrah
Senior Scientist and Technical Advisor
HQAF SPACOM/CN
Peterson AFB, CO 80914-5001

Dr Russ E Davis
Scripps Institution of Oceanography
University of California/San Diego
La Jolla, CA 92093

Dr Gary L Denman
Director
DARPA/DIRO
3701 North Fairfax Drive
Arlington, VA 22203-1714

Dr Nancy Dowdy
USACDA
320 21st Street NW
Washington, DC 20451

DISTRIBUTION LIST

Mr John N Entzminger
Chief, Advance Technology
DARPA/ASTO
3701 North Fairfax Drive
Arlington, VA 22203-1714

Capt Kirk Evans
Director Undersea Warfare
Space & Naval Warfare Sys Cmd
Code PD-80
Department of the Navy
Washington, DC 20363-5100

Dr S William Gouse
Sr Vice President and
  General Manager
The MITRE Corporation
Mail Stop Z605
7525 Colshire Drive
McLean, VA 22102

Dr Michael C Gregg
Applied Physics Laboratory
1013 NE 40th Street
Seattle, WA 98105

Col Randall Gressang
DARPA/DIRO
3701 North Fairfax Drive
Arlington, VA 22203-1714

Mr. Thomas H Handel
Office of Naval Intelligence
The Pentagon
Room 5D660
Washington, DC 20350-2000

Maj Gen Donald G Hard
Director of Space and SDI Programs
Code SAF/AQS
The Pentagon
Washington, DC 20330-1000

Dr Robert G Henderson
Director
JASON Program Office
The MITRE Corporation
7525 Colshire Drive
Mailstop Z561
McLean, VA 22102

Dr Barry Horowitz
President and Chief Exec Officer
The MITRE Corporatior
202 Burlington Road
Bedford, MA 01730-1420

Dr William E Howard I I I [2]
Director of Advanced Concepts &
Systems Design
The Pentagon Room 3E480
Washington, DC 20301-0103

Dr Gerald J Iafrate
U S Army Research Office
PO Box 12211
4330 South Miami Boulevard
Research Triangle NC 27709-2211

J A S O N Library [5]
The MITRE Corporation
Mail Stop W002
7525 Colshire Drive
McLean, VA 22102

Dr George Jordy [25]
Director for Program Analysis
U S Department of Energy
ER30
OER
Washington, DC 20585

Dr O' Dean P Judd
Los Alamos National Lab
Mail Stop A-110
Los Alamos, NM 87545

DISTRIBUTION LIST

Dr Bobby R Junker
Office of Naval Research
Code 111
800 North Quincy Street
Arlington, VA 22217

Mr Robert Madden [2]
Department of Defense
National Security Agency
Attn R-9 (Mr. Madden)
Ft George G Meade, MD 20755-6000

Dr Arthur F Manfredi Jr [10]
OSWR
Central Intelligence Agency
Washington, DC 20505

Mr Joe Martin
Director
OUSD(A)/TWP/NW&M
Room 3D1048
The Pentagon
Washington, DC 20301

Mr James J Mattice
ASAF/Acquisition
SAF/AQ Pentagon
Room 4E-969
Washington, DC 20330-1060

Mr Ronald Murphy
DARPA/ASTO
3701 North Fairfax Drive
Arlington, VA 22203-1714

Dr Julian C Nall
Institute for Defense Analyses
1801 North Beauregard Street
Alexandria, VA 22311

Dr Gordon C Oehler
Central Intelligence Agency
Washington, DC 20505

Dr Peter G Pappas
Chief Scientist
U S Army Strategic Defense Command
PO Box 15280
Arlington, VA 22215-0280

Dr Ari Patrinos
Director
Environmental Sciences Division
ER74/GTN
US Department of Energy
Washington, DC 20585

Dr Bruce Pierce
USD(A)D S
Room 3D136
The Pentagon
Washington, DC 20301-3090

Mr John Rausch [2]
Division Head 06 Department
NAVOPINTCEN
4301 Suitland Road
Washington, DC 20390

Records Resource
The MITRE Corporation
Mailstop W115
7525 Colshire Drive
McLean, VA 22102

Dr Fred E Saalfeld
Director
Office of Naval Research
800 North Quincy Street
Arlington, VA 22217-5000

Dr John Schuster
Technical Director of Submarine
 and SSBN Security Program
Department of the Navy OP-02T
The Pentagon Room ·�"ᴐ534
Washington, DC 20350-2000

DISTRIBUTION LIST